PNNL-13958

Pacific Northwest
National Laboratory
Operated by Battelle for the
U.S. Department of Energy

Thermochemical Optimization of Float Glass Composition: Low-Alumina Glass Development

August 2002

Prepared for the U.S. Department of Energy
under Contract DE-AC06-76RL01830

DISCLAIMER

PACIFIC NORTHWEST NATIONAL LABORATORY
operated by
BATTELLE
for the
UNITED STATES DEPARTMENT OF ENERGY
under Contract DE-ACO6-76RLO183O

Printed in the United States of America

Available to DOE and DOE contractors from the
Office of Scientific and Technical Information,
P.O. Box 62, Oak Ridge, TN 37831-0062;
ph: (865) 576-8401
fax: (865) 576-5728
email: reports@adonis.osti.gov

Available to the public from the National Technical Information Service,
U.S. Department of Commerce, 5285 Port Royal Rd., Springfield, VA 22161
ph: (800) 553-6847
fax: (703) 605-6900
email: orders@ntis.fedworld.gov
online ordering: http://www.ntis.gov/ordering.htm

This document was printed on recycled paper.
(8/00)

PNNL-13958

Thermochemical Optimization of Float Glass Composition: Low-Alumina Glass Development

P. R. Hrma
D. E. Smith
J. D. Yeager
O. P. Lam

August 2002

Prepared for the U.S. Department of Energy
under Contract DE-AC06-76RL01830

Pacific Northwest National Laboratory
Richland, Washington 99352

Abstract

The liquidus temperature (T_L) was measured for a float-glass-type composition region with 72.7 to 74.0 mass% SiO_2, 0.1 to 0.45 mass% Al_2O_3, 8.0 to 9.0 mass% CaO, 3.0 to 4.0 mass% MgO, and 13.1 to 14.2 mass% Na_2O. Crystalline phases were identified at 900°C as cristobalite, wollastonite, and devitrite. The primary phases were tridymite and wollastonite. Partial specific T_Ls were obtained from the data and compared with the literature.

Contents

Figures

Tables

Introduction

Substantial savings can be achieved if low-alumina float glass is produced. It has been proposed to decrease the Al_2O_3 content in the float glass produced by the VGS Glass Systems (VGS) from the original 0.45 mass% to 0.10 mass%. However, the removal of alumina from the current composition must not negatively impact important glass properties, such as viscosity, liquidus temperature (T_L), and chemical durability.

Float glass is essentially a four-component mixture within the SiO_2-Na_2O-CaO-MgO system with minor addition, introduced either deliberately (Al_2O_3, Se_2O_3, Co_3O_4) or as impurities (Fe_2O_3, K_2O). An important processability requirement is that the glass must avoid the tridymite primary phase field. Chemical durability and thermal expansion requirements then place the composition to the neighborhood of the devitrite-wollastonite boundary—see Figure 1. When Al_2O_3 and Fe_2O_3 are present in the mixture, this boundary shifts towards the Na_2O corner of the diagram because Al_2O_3 and Fe_2O_3 bound Na_2O for charge compensation (this allows these oxides to be glass formers).

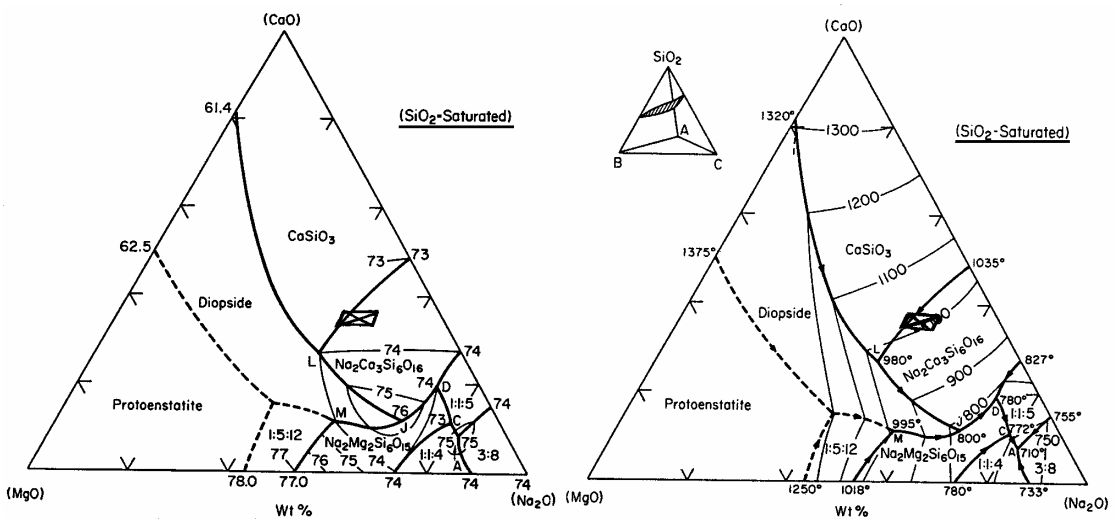

Figure 1. Map of Tridymite Liquidus Surface in Na_2O-CaO-MgO-SiO_2 System; Shahid and Glasser (1972), reproduced in Roth et al. (1981)

Optimizing glass composition with respect glass properties is done most effectively using glass property-composition relationship in the form of simple models. For small composition regions, these models have usually a form of linear functions. Thus, the maximum temperatures (T_j) at which j-th crystals are at equilibrium with glass can be expressed as a function of glass composition using the following relationship:

$$T_j = \sum_{i=1}^{N} T_{ji} x_i \qquad (1)$$

where T_{ji} is the i-th component j-th phase coefficient, x_i is the i-th component mass fraction, and N is the number of components. If N is smaller then the actual number of glass components, mass fractions are normalized in such a way that

$$\sum_{i=1}^{N} x_i = 1 \qquad (2)$$

Several T_L models for commercial glasses exist in the literature. Scholze (1990) reports two such models: Šašek et al. (1973) and Cuartas (1984). Other models were presented by Babcock (1977) and Backman et al. (1997). Component coefficients for these models are summarized in Tables 1 and 2. Table 1 lists component coefficients for linear models represented by Equation (1). Models by Babcock and Šašek et al. are linear in terms of mass fractions of components (x_i). The original model by Cuartas, which is linear in x_i/x_{SiO2}, was converted into the form of Equation (1) by setting $x_{SiO2} = 0.73$. Backman et al.'s (1997) model is nonlinear. Table 2 shows only coefficients relevant for the SiO_2-Na_2O-CaO-MgO-Al_2O_3 system.

Table 1. Component Coefficients T_L in °C

	Babcock[a]					
	Tridymite	Devitrite	Wollastonite	Šašek et al.[a]	Cuartas[b]	Babcock
SiO_2	2324	833	938	1336	1604	1384
Al_2O_3	-7016	2093	3834	304	2533	1459
Fe_2O_3				8936	1229	
CaO	-342	3061	3307	4349	2060	2365
MgO				-1225	89	
Na_2O	-4115	69	-765	-2105	-2756	-1619
K_2O				3096	-2200	

[a] Babcock's and Šašek et al.'s models were transformed to the form of Equation (1); the resulting coefficients are shown.

[b] Cuartas' coefficients were adjusted to float glass region with 73 mass% SiO_2.

Table 2. Component Coefficients T_L in °C in the Nonlinear Model by Backman et al.[a]

	(°C/mass%)
Intercept	8.90E+02
CaO	3.07E+01
$Na_2O \times Na_2O$	-1.83E+00
$Al_2O_3 \times Na_2O$	2.69E+00
$Na_2O \times CaO \times MgO$	2.83E -01
$CaO \times CaO \times MgO \times MgO$	-5.30E -02
$Na_2O \times Na_2O \times Na_2O \times Na_2O$	2.10E -03

[a] Only coefficients applicable to the VGS composition region are shown.

Unfortunately, the usefulness of T_L coefficients that cover multiple primary phase fields is rather dubious. Because the effect of glass components on T_L substantially, even dramatically, changes from one primary phase to another, the global models have a significant lack of fit. Global polynomial forms only partly remedy the problem. In addition, polynomial models cannot be extrapolated beyond their experimental domain.

Generally, it is not recommended to apply models beyond the composition region of their validity. Composition regions of the literature models are compared with the float-glass composition region in Table 3. Babcock used Silverman's (1939) data and a large database available at Owens-Illinois laboratories. Babcock does not provide the composition region of his Owens-Illinois data. Therefore, only the composition region of Silverman's study is shown in Table 3.

Table 3. Composition Regions for VGS Glasses and for Published Models (mass%)[(a)]

	Float		Experimental		Šašek et al. (1973)		Cuartas (1984)		Backman (1997)		Silverman (1939)	
	min	max	min	max	min	max	min	max	min	max	min	max
SiO_2	67.5	77.2	72.7	74	69.4	76	64.9	73.1	50.2	68.2	59	79
Al_2O_3	0.1	2	0.1	0.45	0.3	0.5	0.4	4	0.5	3	0.2	8.2
Fe_2O_3	0.1	1.5	0.7	0.7	0	0.5	0	0.9	0	0	0	0
CaO	7	9	8	9	7	8.5	6.6	12.2	2.7	14.2	6	18
MgO	3	4	3	4	2.5	4.5	0.1	4.9	0.5	5	0.2	0.2
Na_2O	12	15	13.1	14.2	13	16	11.8	14.8	8.4	22.9	11	17
K_2O	0	2	0.03	0.1	0	0.5	0.1	2.3	0.5	7		

[(a)] Values are highlighted yellow/green where maximum/minimum values of component ranges were lower/higher than the corresponding maximum/minimum of the experimental range.

Experimental

A test matrix of 14 glasses, shown in Table 4, was developed by the VGS project.

Table 4. Test Glass Compositions in Mass% of Oxides

High Al_2O_3 (mass%)	Standard	Low CaO	High CaO	Low MgO	High MgO	Low Na_2O	High Na_2O
SiO_2	**73.18**	**73.68**	**72.68**	**73.68**	**72.68**	**73.68**	**72.68**
Al_2O_3	**0.45**	0.45	0.45	0.45	0.45	0.45	0.45
TiO_2	**0.01**	0.01	0.01	0.01	0.01	0.01	0.01
Fe_2O_3	**0.71**	0.71	0.71	0.71	0.71	0.71	0.71
CaO	**8.45**	**7.95**	**8.95**	8.45	8.45	8.45	8.45
MgO	**3.47**	3.47	3.47	**2.97**	**3.97**	3.47	3.47
Na_2O	**13.63**	13.63	13.63	13.63	13.63	**13.13**	**14.13**
K_2O	**0.10**	0.10	0.10	0.10	0.10	0.10	0.10
Sum	100.00	100.00	100.00	100.00	100.00	100.00	100.00

Low Al_2O_3 (mass%)	Standard	Low CaO	High CaO	Low MgO	High MgO	Low Na_2O	High Na_2O
SiO_2	**73.53**	**74.03**	**73.03**	**74.03**	**73.03**	**74.03**	**73.03**
Al_2O_3	**0.10**	0.10	0.10	0.10	0.10	0.10	0.10
TiO_2	**0.01**	0.01	0.01	0.01	0.01	0.01	0.01
Fe_2O_3	**0.71**	0.71	0.71	0.71	0.71	0.71	0.71
CaO	**8.45**	**7.95**	**8.95**	8.45	8.45	8.45	8.45
MgO	**3.47**	3.47	3.47	**2.97**	**3.97**	3.47	3.47
Na_2O	**13.70**	13.70	13.70	13.70	13.70	**13.20**	**14.20**
K_2O	**0.03**	0.03	0.03	0.03	0.03	0.03	0.03
Sum	100.00	100.00	100.00	100.00	100.00	100.00	100.00

The test matrix consists of two standard glasses one for high-alumina (0.45 mass%) glass and the other for low-alumina (0.10 mass%) glass. Both standards are equal in Al_2O_3+SiO_2 content and in Na_2O+K_2O content (the K_2O content is 0.10 mass% in the high-alumina standard glass and 0.03 mass% in the low-alumina standard glass. The remaining glasses are derived from the standard glasses by one-at-a-time changes in CaO, MgO, and Na_2O. These changes are compensated for by equal changes in the SiO_2 fraction. The composition regions covered by the VGS test matrix is shown as the experimental region in Table 3 and represented by a parallelogram in Figure 1.

As evident form Table 3, Šašek et al.'s (1973) composition region is broader than the experimental composition region, except for Al_2O_3. The Cuartas (1984) composition region is wider than Šašek's composition region, except for the upper limit for the range of SiO_2. Backman et al. (1997) studied glasses with the SiO_2 content <68.2 mass%. Their glasses also had at least 0.5 mass% of each of the following oxides: Al_2O_3, K_2O, B_2O_3, SrO, and BaO. Composition regions in these studies covered several primary phase fields, including tridymite, devitrite, wollastonite, and other phases, such as diopside.

Because the composition variations are small (see bold numbers in Table 4), careful preparation of glasses and precise measurements of the T_L were required. Batches were prepared from chemicals listed in Table 5.

Table 5. Source Chemicals

Chemical	Manufacturer	Lot Number
Al_2O_3	Fisher	006627
$CaCO_3$	Fisher	007112
Fe_2O_3	Fisher	005612
K_2CO_3	Aesar	031384
MgO	Aldrich	08629JF
Na_2CO_3	Fisher	006825
SiO_2	Fisher	010455
TiO_2	J.T. Baker	525355

The chemicals were weighed to obtain batches for 250-g glass. Batches were blended, first by hand in a plastic bag (roll and shake), and then milled in an agate disc mill for 2 min. The glass was melted twice, each time in a Pt-10%Rh crucible for 1 h at 1450°C. After the first melt, the glass was hand crushed and then milled in a tungsten carbide disc mill for 2 min.

The T_L was measured in a gradient temperature furnace. Pt boats filled with crushed glass (between 20 and 40 mesh size) were heat treated for 24 h in the temperature gradient of 1.0°C/mm, spanning the temperature interval from 800°C to 1050°C. Rods of heat-treated glass were mounted in epoxy, and the portion exposed to T >936°C was thin-sectioned for microscopic evaluation.

To identify phases, approximately 2.5-g samples of each glass were heat-treated in a Pt crucible for 24 h at 900°C. X-ray diffraction (XRD) was performed on these samples (using Scintag DMC-008) to detect the crystalline phases present and to measure their concentrations. CaF_2 (5 mass%) was added to the samples as the standard to evaluate fractions of crystalline phases. Jade software was used for the analysis.

Results

XRD analysis detected three phases in the samples: cristobalite (SiO_2), devitrite ($Na_2O{\cdot}3CaO{\cdot}6SiO_2$), and wollastonite ($CaO{\cdot}SiO_2$) (Figure 2). Table 6 shows the fractions of these phases in the glasses at 900°C. The visual appearances of crystals of these phases were identified using both XRD data and the literature (Bartuška 2001). Using the optical microscope (Olympus PMG-3), the maximum temperatures (T_j) at which j-th crystals were observed in the thin sections were determined (Table 7); typical examples are shown in Figures 3 to 11. The T_Ls (the highest T_j) are shown in bold in Table 7.

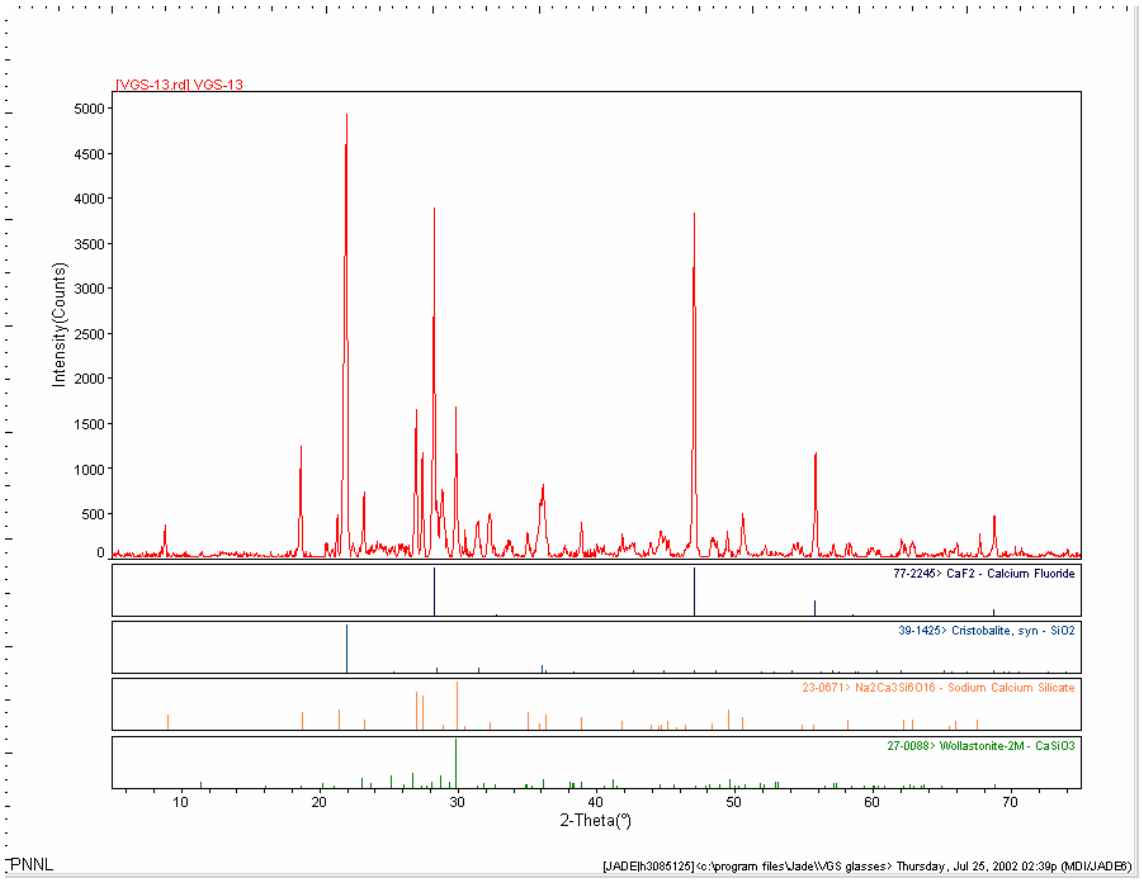

Figure 2. XRD Pattern of Low-Al_2O_3-Low-Na_2O Glass Heat-Treated at 900° C for 24 h

Table 6. Mass Fractions of Crystalline Phases in Glasses Heat-Treated at 900° C for 24 h

	Cristobalite	Devitrite	Wollastonite
High Al_2O_3			
Standard	0.033	0.060	-
Low CaO	0.041	-	-
High CaO	-	0.061	0.043
Low MgO	0.045	0.047	-
High MgO	-	0.061	0.061
Low Na_2O	0.072	0.076	0.076
High Na_2O	0.020	0.079	-
Low Al_2O_3			
Standard	0.052	0.066	-
Low CaO	0.071	0.046	-
High CaO	0.061	0.129	-
Low MgO	0.055	0.067	-
High MgO	0.031	0.057	-
Low Na_2O	0.072	0.079	0.092
High Na_2O	0.027	0.055	-

Table 7. Maximum Temperatures (°C) at Which Individual Crystalline Phases Occurred in VGS Glasses[a][b]

	Tridymite	Devitrite	Wollastonite	T_L
High Al_2O_3				
Standard		967	**992**	**992**
Low CaO	**990**	952	973	**990**
High CaO		973	**1011**	**1011**
Low MgO	**997**	962	980	**997**
High MgO		975	**1001**	**1001**
Low Na_2O	**1011**	971	998	**1011**
High Na_2O		965	**989**	**989**
Low Al_2O_3				
Standard	**995**	965	977	**995**
Low CaO	**1024**	968	968	**1024**
High CaO		965	**1000**	**1000**
Low MgO	**1026**	970	980	**1026**
High MgO		965	**994**	**994**
Low Na_2O	**1044**[c]	962	990	**1044**
High Na_2O		970	**979**	**979**

[a]936°C was the minimum temperature at which glasses were evaluated.

[b]Bold numbers indicate T_L (see also the last column)

[c]1044°C was the maximum temperature at which glasses were evaluated; repeated tests showed that this was also the T_L value for the low-Al_2O_3-low-Na_2O glass.

Figure 3. Crystals of Cristobalite in Low-Al_2O_3-Low-CaO Glass, 1020°C

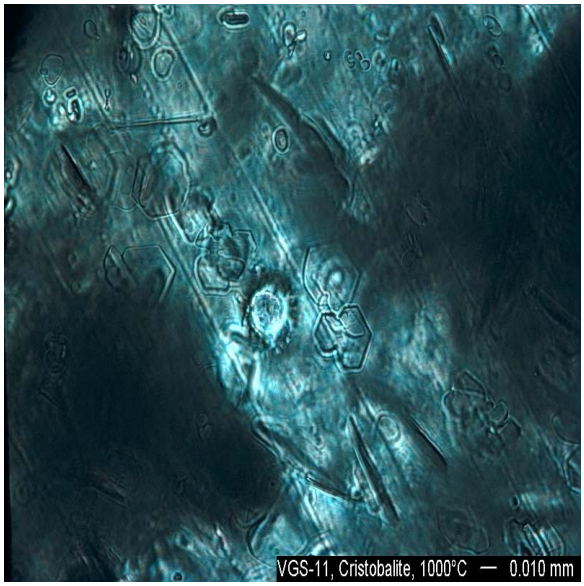

Figure 4. Crystals of Cristobalite in Low-Al_2O_3-Low-MgO Glass, 1000°C

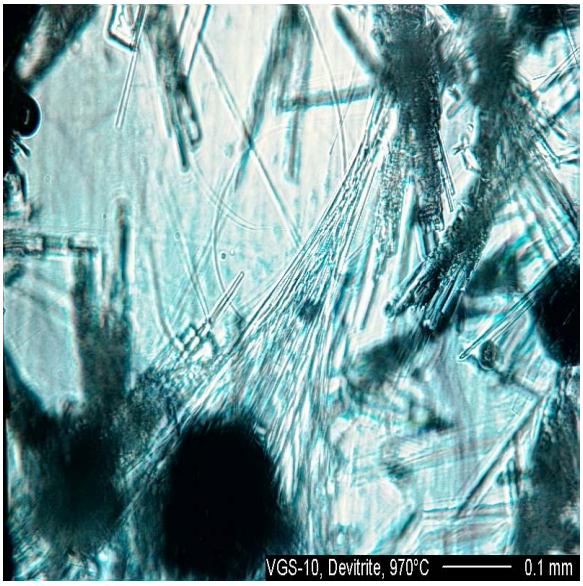

Figure 5. Crystals of Devitrite in Low-Al_2O_3-High-CaO Glass, 970°C

Figure 6. Crystals of Devitrite in Low-Al_2O_3-High-MgO Glass, 965°C

Figure 7. Crystals of Wollastonite in Low-Al_2O_3-High-CaO Glass, 995°C

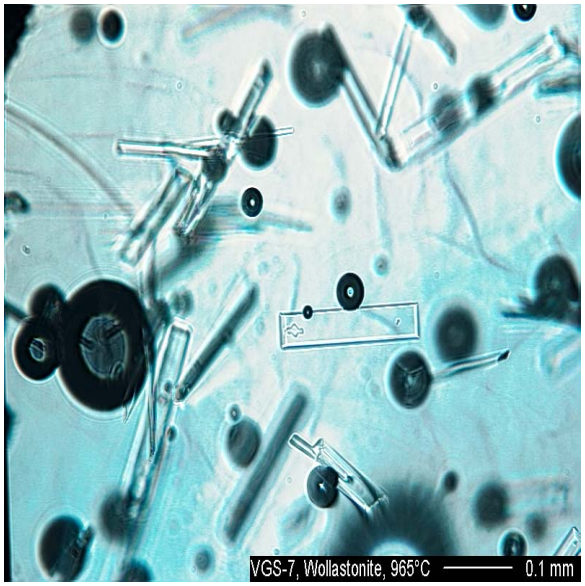

Figure 8. Crystals of Wollastonite in High-Al_2O_3-High-Na_2O Glass, 965°C

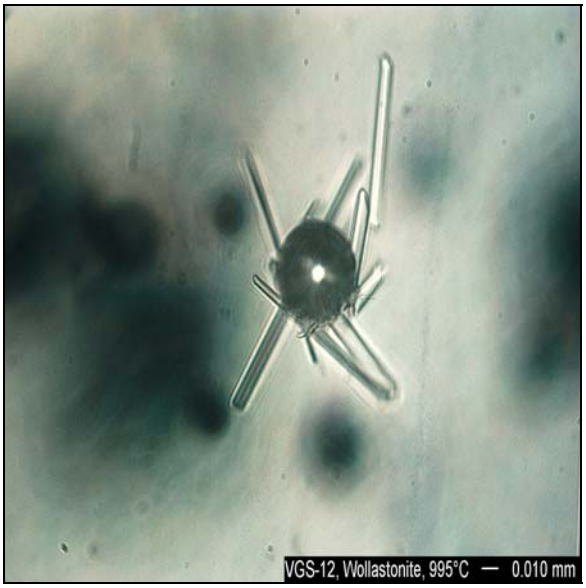

Figure 9. Crystals of Wollastonite, Nucleated on a Bubble, in Low-Al_2O_3-High-MgO Glass, 995°C

Figure 10. Crystals of Wollastonite and Probably Devitrite, Nucleated on a Bubble, in High-Al_2O_3-Baseline Glass, 975°C

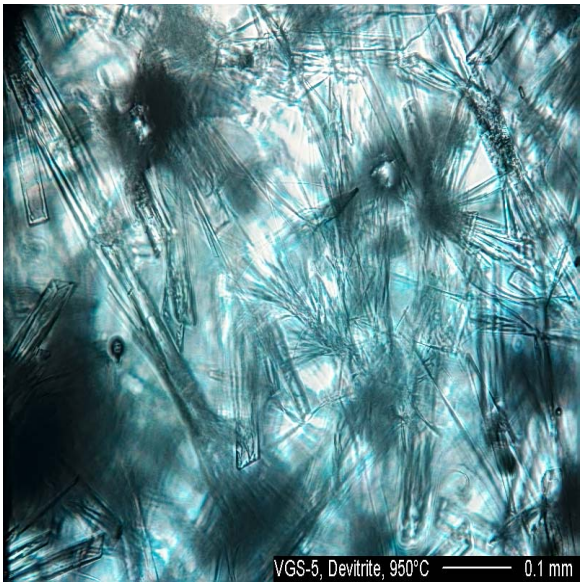

Figure 11. Crystals of Devitrite and Wollastonite in High-Al_2O_3-High-MgO Glass, 950°C

Discussion

Figures 12 to 14 show that T_j is a nearly linear function of composition. To fit Equation (1) to data, mass fractions were normalized to the following five components: SiO_2, Na_2O, CaO, MgO, and Al_2O_3. The resulting coefficient values are listed in Table 8. The T_j values calculated with these coefficients, using Equation (1), are compared with measured T_js in Figure 15.

Table 8. Component Coefficients (T_{ji}) for the Maximum Temperatures at which Tridymite, Devitrite, Wollastonite Occur in Float Glasses at Equilibrium (in °C)[(a)]

	Tridymite	Devitrite	Wollastonite	T_L
SiO_2	3033	863	763	1669
Al_2O_3	-7560	862	2787	-1936
CaO	-2525	1756	4235	1521
MgO	-3418	1260	2499	281
Na_2O	-6593	962	-230	-2646
R^2	0.997	0.233	0.950	0.608
adjR^2	0.991	-0.108	0.927	0.434
s	1.9	6.0	3.3	13.2
n	7	14	14	14

[(a)]The coefficients are valid for the experimental composition region shown in Table 3. Note that the effect of Al_2O_3 is compounded with the effect of K_2O replacing Na_2O. The symbols on the two bottom lines: s is the standard error, and n is the number of observations.

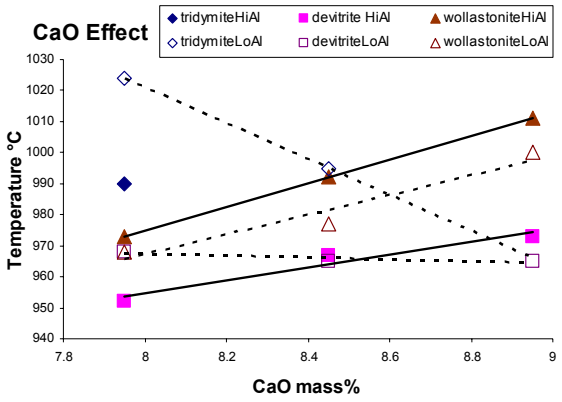

Figure 12. The Effect of CaO on the Maximum Temperature at which Tridymite, Devitrite, and Wollastonite occur in Float Glass at Equilibrium

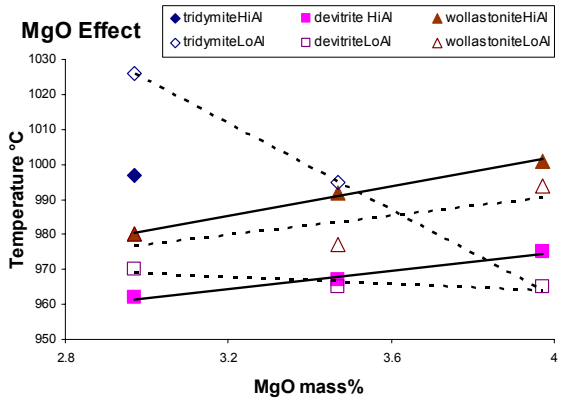

Figure 13. The Effect of MgO on the Maximum Temperature at which Tridymite, Devitrite, and Wollastonite Occur in Float Glass at Equilibrium

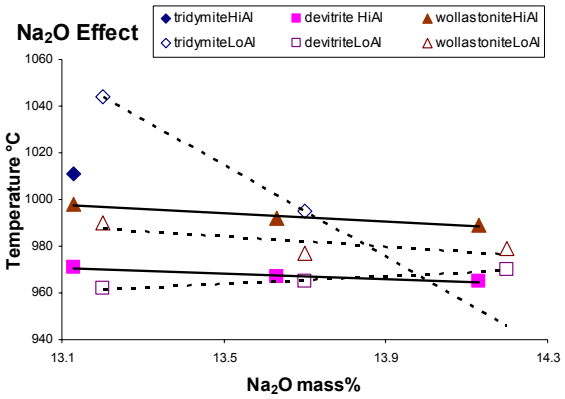

Figure 14. The Effect of Na_2O on the Maximum Temperature at Which Tridymite, Devitrite, and Wollastonite Occur in Float Glass at Equilibrium

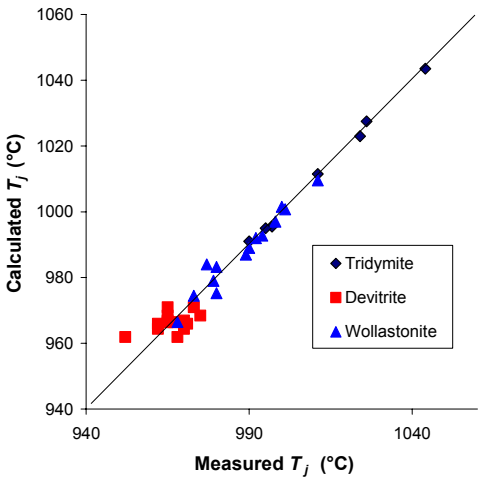

Figure 15. T_j , Calculated vs. Measured

At 900°C, the crystalline form of silica as detected by XRD was cristobalite (Figure 2). At temperatures below 1470°C, the stable form of silica in soda-lime glasses is tridymite; however, as reported by Bartuska (2001), cristobalite occurs in industrial glasses at lower temperatures, alone or together with tridymite. No attempt was made to distinguish between these two forms in this study. However, we assume that tridymite was the primary phase.

As Table 7 shows, tridymite was the primary phase in all glasses in which the SiO_2 content was >75.3 mass%. In all other glasses, the primary phase was wollastonite. In these glasses cristobalite did not form at T >936°C, but was detected in some glasses that were heat-treated at 900°C (Table 6). Devitrite and wollastonite were found in all glasses, though wollastonite disappeared at lower temperatures and was not detected at 900°C in most glasses (Table 6). The highest temperature at which devitrite was observed was virtually independent of composition. It varied within a narrow temperature interval of 950°C to 975°C, but these variations in T_j cannot be explained in terms of composition variation: note the low R^2 value for $T_{devitrite}$ in Table 8.

Table 8 shows that the $T_{cristobalite}$ increases with SiO_2 fraction and decreases with the addition of any other component, most notably Al_2O_3 and Na_2O. The formation of wollastonite is promoted mainly by CaO, but also by MgO and Al_2O_3, whereas NaO_2 suppresses its formation. The component coefficients for tridymite and wollastonite are much different for each component, showing that the slopes of the corresponding liquidus surfaces are substantially different and even opposite in Al_2O_3, CaO, and MgO components. Therefore, the linear model for T_L (the last column in Table 8) is not a good representation of the real behavior. This is well illustrated in Figures 12 to 14.

The low-Al_2O_3 standard glass is close to the boundary between the tridymite and wollastonite primary phases. Its T_L is only 3°C higher than that of the high-Al_2O_3 standard; this difference is within the standard deviation for T_{ji} of wollastonite (Table 8). It is, however, possible to decrease low Al_2O_3 glass T_L by changing the MgO-to-CaO ratio.

Figures 16 and 17 compare T_j and T_L measured values with those calculated using different models. It is not surprising, as seen in Figure 17, that linear or polynomial models are subjected to a large error.

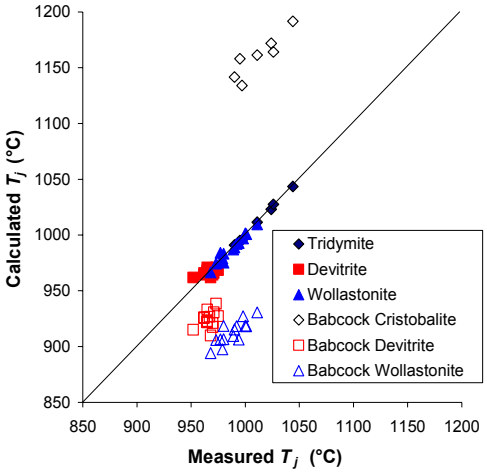

Figure 16. Comparison of Experimental T_j Values for VGS Glass with Babcock's T_L Values for Soda-Lime Glass

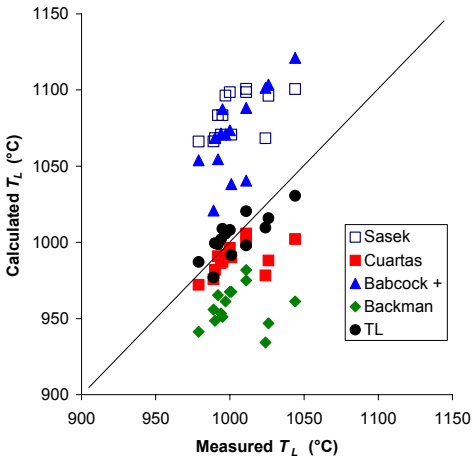

Figure 17. Comparison of Experimental T_L Values for VGS Glass with T_L Values Predicted by Various Models

Using Babcock's coefficients, T_j values were predicted for experimental compositions normalized to the Na_2O-CaO-SiO_2 system. As seen in Figure 16, Babcock's models overestimate T_j values for tridymite and underestimate T_j values for devitrite and wollastonite. These differences can be attributed to the effect of MgO in the experimental glasses.

As a comparison of the coefficients in Table 8 with those in Table 1 shows, Cuartas' coefficients are closer to our empirical coefficients than those by Šašek et al. (1973). Hence, even though Šašek et al.'s (1973) composition region is closer to our experimental composition region than that of Cuartas (1984), T_L values from Šašek et al.'s model less closely match the experimental T_Ls (Figure 17).

The main cause of the difference between our Al_2O_3 coefficients for T_L and those by other authors is probably the confounding between substituting SiO_2 for Al_2O_3 together with substituting K_2O for Na_2O. Our Al_2O_3 coefficient accounts for this four-component change and thus cannot be compared with studies in which the Al_2O_3 fraction was an independent variable. Another factor is the extremely narrow range of Al_2O_3 content in our study (0.10 to 0.45 mass% as compared to 0.2 to 8.2 mass% of Silverman [1939]).

The experimental composition region of this study is shown in Figure 1 as a parallelogram. Figure 1 displays isotherms and SiO_2 fractions on the SiO_2 saturation surface in the Na_2O-CaO-MgO-SiO_2 system. When the experimental glasses are normalized to this four-component system, the SiO_2 mass fraction varies from 0.737 to 0.747. Glasses with tridymite primary phase are those with a SiO_2 mass fraction higher than 0.741 (within the Na_2O-CaO-MgO-SiO_2 system). This is in excellent agreement with SiO_2 contours in Figure 1.

Figure 1 suggests that glasses outside of the tridymite primary phase field are located in the devitrite primary phase field, whereas the experimental glasses had wollastonite as their primary phase. As mentioned earlier, this shift was probably caused by Fe_2O_3 and Al_2O_3 in the experimental glass. These two oxides become network formers by immobilizing Na^+ ions. Therefore, the effective Na_2O content is

lower in the experimental glasses, which would shift the experimental composition region into the wollastonite fields.

Conclusions

Low-alumina the standard glass has nearly identical T_L (995°C) as the high-alumina the standard glass (992°C). Its primary phase is tridymite, while wollastonite is the primary phase of the latter glass. Decreasing SiO_2 fraction by as little as 0.3 mass% (by replacing it with CaO, MgO, Na_2O, or their combination) shifts the glass into the wollastonite primary phase field. While in this field, the secondary phase is devitrite.

Neither of the two standard glasses contains wollastonite when equilibrated at 900°C; both contain cristobalite and devitrite, the low-alumina glass at somewhat higher fraction. This, however, should not be a problem in float glass manufacturing.

The effects of SiO_2, CaO, MgO, and Na_2O on the T_L within each primary phase field were expressed as partial-specific T_Ls. These coefficients allow a further optimization on the low-alumina glass.

The partial-specific T_L coefficients published in the literature do not predict the T_L values satisfactorily. It appears that two conditions are necessary for a correct prediction of T_L: 1) separate models are developed for each primary phase field and 2) the major components of the model are the same as the major components of the composition region of interest.

References

Babcock CL. 1977. *Silicate Glass Technology Methods*. John Wiley, New York.

Backman R, KH Karlsson, M Cable, and NP Pennington. 1997. "Model for Liquidus Temperature of Multi-Component Silicate Glasses." *Physics and Chemistry of Glasses* 38, 103-109.

Bartuška M. 2001. "Crystalline Inclusions." In *Glass Flaws* (in Czech), Bartuška M, Editor, Práh, Prague, Czech Republic.

Cuartas R. 1984. "Calculo teorico de propiedades del vidrio: viscosidad, parametros termicos y parametros de desvitrificacion." *Ceram*. *Vidrio* 23, 105-111.

Roth RS, T Negas, and LP Cook. 1981. *Phase Diagrams for Ceramists*. Volume IV. American Ceramic Society, Columbus, Ohio.

Šašek L, M Bartuška, and V Van Thong. 1973. "Utilization of Mathematico-Statistical Methods in Silicate Research. 2. Determination of Mathematical Relations for the Calculation of Crystallization Properties from Chemical Composition of Sheet and Container Glass" (in Czech). *Silikaty* 17, 207-217.

Scholze H. 1990. *Glass Nature, Structure, and Properties*. Springer, New York.

Shahid KA and FP Glasser. 1972. *Physics and Chemistry of Glasses* 13, 27 (referenced in Roth et al. 1981).

Silverman WB. 1939. "Effect of Alumina on Devitrification of Soda-Lime-Silica Glasses." *Journal of the American Ceramics Society* 22, 378-384.

Distribution

No. of Copies

OFFSITE

1 James V. Jones
Technical Fellow
Advanced Technology and Engineering
Visteon Glass System
15000 Commerce Drive
N. Dearborn, MI 48120

3 Edward N. Boulos, Ph.D. (3)
Senior Technical Fellow
Advanced Technology and Engineering
Visteon Corporation
Visteon Glass System
15000 Commerce Drive
N. Dearborn, MI 48120

1 Dr. Theodore M. Besmann, Head
Surface Processing and Mechanics Group
Oak Ridge National Laboratory
1 Bethel Valley Road
P.O. Box 2008
Oak Ridge, TN 37831-6063

No. of Copies

ONSITE

10 Pacific Northwest National Laboratory

D-S Kim	K6-24
J. D. Vienna	K6-24
P. R. Hrma (7)	K6-24
M. A. Khaleel	K2-18